Available online at www.sciencedirect.com
SCIENCE DIRECT®
Journal of Nuclear Materials 350 (2006) 203–207
journal of nuclear materials
www.elsevier.com/locate/jnucmat

Characterization of simulated burnup fuel by nanoindentation

Ken Kurosaki *, Yoshiyuki Saito, Masayoshi Uno, Shinsuke Yamanaka

Division of Sustainable Energy and Environmental Engineering, Graduate School of Engineering, Osaka University, 2-1 Yamadaoka, Suita, Osaka 565-0871, Japan

Received 14 May 2005; accepted 5 January 2006

Abstract

A simulated burnup UO_2 based fuel (150 GWd/t) was prepared by solid-state reactions. The phase equilibria of the simulated fuel were evaluated by XRD and SEM/EDX analysis. Nanoindentation tests were performed for the simulated fuel at room temperature in air. The modulus and hardness of the matrix phase and oxide precipitates that exit in the simulated fuel were directly evaluated by the nanoindentation.

PACS: 62.20

1. Introduction

An actual irradiated fuel is in extreme situations such as a high radiation field and a large temperature gradient, which leads to the complicated phase relation and microstructure. In addition, a lot of fission product (FP) elements are produced and accumulated under irradiation, and they have a great influence on the thermal and mechanical properties of an irradiated fuel. In order to evaluate the effect of FP elements on the physical properties of the fuel, a concept of simulated burnup fuel that contains non-radioactive solid-state FP elements has been proposed.

The simulated burnup fuel is a material that replicates the chemical states and phase relation of the irradiated fuel. Ordinarily, the simulated fuel is composed of the matrix phase and precipitates [1–3]. In the matrix phase, the actinide and rare earth elements are incorporated as solid solutions. The majority of Ba and Sr appears to be the oxide precipitates as a perovskite-type oxide with the chemical form of $(Ba,Sr)(U,Zr,Mo)O_3$. The metallic precipitates mainly consist of Mo, Tc, Ru, Rh, and Pd. The composition of the phases is affected by the circumstance in the fuel, especially the oxygen potential.

Previous investigations on the simulated fuel have examined the phase equilibria [1–3], the effect of the oxygen potential on the crystalline structure [4], and the thermal conductivity [5], etc. Recently, Lucuta et al. [5] and Matzke et al. [6] have studied the effect of the fission product (FP) elements on the thermophysical and thermochemical properties

* Corresponding author. Tel.: +81 6 6879 7905; fax: +81 6 6879 7889.
E-mail address: kurosaki@nucl.eng.osaka-u.ac.jp (K. Kurosaki).

0022-3115/$ - see front matter © 2006 Elsevier B.V. All rights reserved.
doi:10.1016/j.jnucmat.2006.01.005

of the simulated fuel with equivalent simulated burnups of 3 at.% (corresponding to 28 GWd/t) and 8 at.% (corresponding to 75 GWd/t).

On the other hand, the nanoindentation technique [7–11] has been developed in some decades, and the mechanical properties within a sub-micron or nanoscale are widely discussed. The techniques are expected to be useful for measurement of the mechanical properties of thin films or local structure of various materials. However, there are few attempts of applying the nanoindentation to evaluate the mechanical properties of the nuclear fuels and materials. In our previous studies [12,13], we have performed the nanoindentation tests for UO_2 and some other oxide ceramics, and evaluated the nanoscale mechanical properties.

In the present study, the nanoindentation tests are performed for the simulated fuel. The nanoindentation test enables us to evaluate directly the modulus and hardness of the matrix phase and oxide precipitates that exist in the simulated fuel.

2. Experimental

The simulated fuel with a burnup of 150 GWd/t was prepared. The composition of the simulated fuel was determined using ORIGEN-2 code [14] as shown in Table 1. Appropriate amounts of high-purity oxides of the representative FP elements were mechanically mixed with UO_2 powder and calcined at 2023 K in reduction atmosphere (under $H_2 + N_2$ gas flow condition). The powder thus obtained was pressed into a pellet under a uniaxial pressure. The pellet was annealed at 1400 K for 18 h under an oxygen potential of −390 kJ/mol.

Table 1
Composition of the simulated fuel with the burnup of 150 GWd/t

6.2 wt%-U235	Simulated burnup: 150 GWd/t (15.47 at.%)	
Representative elements	mol%	wt%
U	78.90	88.48
Ba	1.944	1.257
Zr	3.227	1.387
Mo	3.655	1.652
Ru	2.688	1.280
Rh	0.140	0.068
Pd	2.108	1.057
Y	0.392	0.164
La	1.147	0.751
Ce	1.797	1.186
Nd	3.998	2.716
Total	100.00	100.00

The phase equilibria of the simulated fuel were examined by XRD (Cu-Kα radiation) and SEM/EDX analysis. The oxygen and metal (O/M) ratio of the sample was identified to be 2.001, which was evaluated using an oxygen analyzer HORIBA EMGA-550. The sample bulk density was evaluated to be 8.58 g/cm^3, which corresponds to 88% of the theoretical density (12% porosity). The average grain size of the sample was several μm.

For the nanoindentation tests, the sample was formed to a disc-shape with the diameter of 10 mm and thickness of 1.0 mm. The surface of the sample was polished with 0.3 μm-diamond powders to a mirror-like surface.

The nanoindentation tests were performed at room temperature in air using an atomic force microscope (AFM) supplied by JEOL (JSPM-4200) with a nanoindenter named TriboScope (Hysitron Inc.). From load–displacement curves obtained by the nanoindentation tests, the reduced modulus E_r and nanohardness H_n can be evaluated by a method suggested by Oliver and Pharr [7]. The reduced modulus E_r can be combined with the modulus of a specimen and an indenter by the following relationship [7]:

$$\frac{1}{E_r} = \frac{1 - v_s^2}{E_s} + \frac{1 - v_i^2}{E_i}, \quad (1)$$

where E and v are the Young's modulus and Poisson's ratio, and the subscripts s and i represent the sample and indenter, respectively. Assuming that the value of $E_i = 1140$ GPa and $v_i = 0.07$ for the diamond indenter, and $v_s = 0.25$ for the sample, E_s is about 15% higher than E_r.

In order to obtain the accurate relationship between the indentation depth and projected contact area, it is necessary to perform the tip shape calibration based on a method suggested by Oliver and Pharr [7]. In the present study, to determine the area function, a series of the indentations at the various contact depths corresponding to the load of 2500–3500 μN were performed on the standard sample (fused SiO_2). The load of 3000 μN was applied for the nanoindentation tests for the simulated fuel.

3. Results and discussion

Fig. 1(a) shows the XRD pattern of the simulated fuel for the burnup of 150 GWd/t annealed under the oxygen potential of −390 kJ/mol. There are

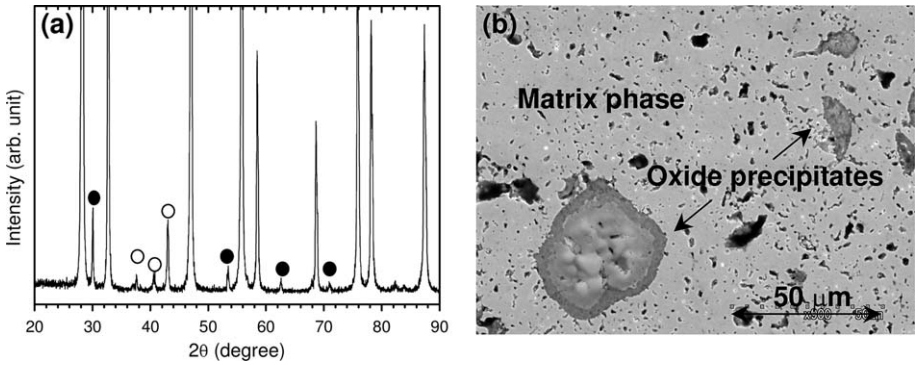

Fig. 1. (a) X-ray diffraction pattern of the simulated fuel, (b) SEM image of the simulated fuel surface after polishing. The simulated burnup is 150 GWd/t. The fuel was annealed under the oxygen potential of −390 kJ/mol. In the XRD pattern, the open and solid circles represent Mo–Me (Me: Ru, Rh, Pd) alloy and $BaMO_3$ (M: U, Zr, Mo), respectively. The other peaks correspond to those of the matrix phase.

some peaks corresponding to the matrix phase (fluorite type structure), oxide inclusion (perovskite-type structure), and metallic inclusion (ε-phase). Fig. 1(b) shows the SEM image of the simulated fuel surface after polishing. It is observed that the oxide precipitates exist on the surface. The metallic precipitates cannot be observed in this figure because the magnification is too small to confirm them. From the XRD and EDX analysis, it is considered that the oxide and metallic inclusions form a perovskite-type oxide phase '$Ba(U, Zr, Mo)O_3$' and an ε-phase 'Mo–Ru–Rh–Pd alloy', respectively.

Fig. 2(a) shows the AFM image of the simulated fuel surface. A triangle shaped trace with the side length of approximately 500 nm and the depth of approximately 100 nm is observed. Since the size of the oxide precipitates is around 20 μm as shown in Fig. 1(b) that is extremely larger than the size of the nanoindentation trace, it appears to be possible to perform the indentation only for the oxide precipitates and evaluate directly their mechanical properties.

Fig. 2(b) shows the load–displacement curves obtained from the nanoindentation performed on the simulated fuel surface. In the present study, the nanoindentation was performed randomly around a hundred times. It can be seen that there are two patterns in the load–displacement curves, one is shown by solid lines and the other is shown by dashed lines. The number of the solid curves is about 90% of all the curves. It has been confirmed from the SEM/EDX analysis that about 90% of the surface area of the simulated fuel is the matrix phase, and about 10% of that is the oxide precipitates. Therefore, it is decided that the solid curves represent the matrix phase, and the dashed curves represent the oxide precipitates.

The reduced modulus and nanohardness of the matrix phase and oxide precipitates were calculated from the load–displacement curves. The calculated

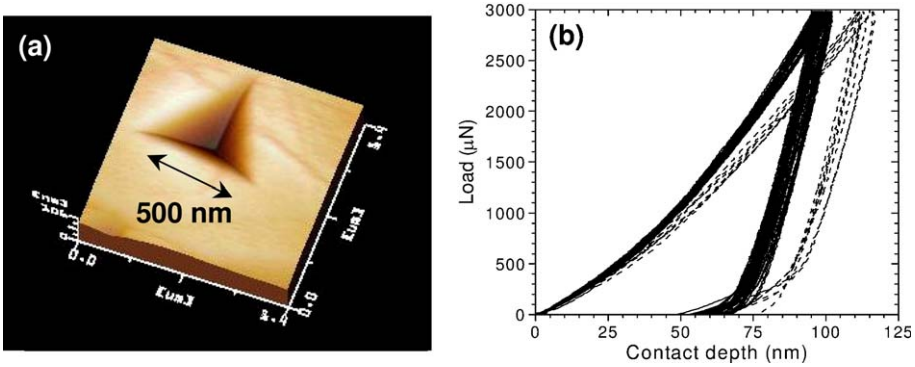

Fig. 2. (a) AFM image of the indentation trace, (b) load–displacement curves for the simulated fuel.

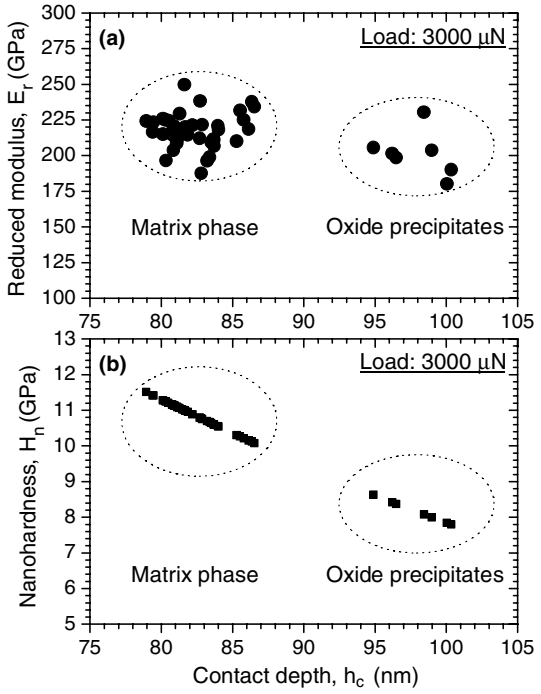

Fig. 3. (a) Reduced modulus and (b) nanohardness of the simulated fuel as a function of contact depth.

reduced modulus and nanohardness as a function of the contact depth are shown in Fig. 3(a) and (b), respectively. Both the reduced modulus and nanohardness of the matrix phase are higher than those of the oxide precipitates. The indentation size effect is cleanly observed in the relationship between the nanohardness and contact depth. It has been reported that the nanohardness decreases with increasing the indentation depth; for instance, the indentation size effects for aluminum, titanium single crystal, and silicon single crystal have been reported by Oliver and Pharr [7], Mante et al. [15], and Page et al. [16], respectively. In general, the indentation hardness of a material is observed to increase with decreasing size of indentation owing to the nucleation of dislocations within the plastic zone. Nix and Gao show that the indentation size effect is related to geometrically necessary dislocations (GNDs), whose density is proportional to the inverse indentation depth [17].

The mean values of the reduced modulus and nanohardness of the matrix phase are 217 ± 20 GPa and 10.9 ± 1.5 GPa, respectively. The mean values of the reduced modulus and nanohardness of the oxide precipitates are 197 ± 17 GPa and 8.2 ± 0.5 GPa, respectively. The reduced modulus for the matrix phase is slightly lower than that of polycrystalline UO_2 measured in the author's group, in which the value of the reduced modulus is 223 ± 7 GPa [12]. The modulus of the polycrystalline UO_2 is the value measured by the nanoindentation that appears not to be affected by the pellet porosity. Therefore, this lower elastic modulus of the matrix phase than that of UO_2 appears to be caused by the dissolution of the FP elements such as rare earth elements. For example, it has been reported that the Young's modulus of 10 wt%Gd_2O_2 doped UO_2 is approximately 5% lower than that of UO_2 [18]. In addition, the present authors have confirmed that the Young's modulus of $(U,Ce)O_2$ measured by the ultrasonic pulse echo method decreases with increase of CeO_2 content [19]. The values of the nanoscale mechanical properties of the simulated fuel and UO_2 [12] are summarized in Table 2.

Table 2
Values of the nanoscale mechanical properties of the simulated fuel and UO_2 [12]

		Reduced modulus E_r (GPa)	Nanohardness H_n (GPa)
Simulated fuel (150 GWd/t)	Matrix phase	217 ± 20	10.9 ± 1.5
	Oxide inclusion	197 ± 17	8.2 ± 0.5
Polycrystalline UO_2 pellet [12]		223 ± 7	8.5 ± 0.4

In the present study, we have evaluated the nanoscale mechanical properties of the simulated fuel using the nanoindentation technique. The nanoindentation test enables in situ measurement of the mechanical properties of the matrix phase and oxide precipitates existed in the simulated fuel surface. It is possible that the nanoindentation test can be applied to post irradiation examinations, because the system and apparatus are enough small and simple to use in a hot cell. It is expected that the nanoindentation becomes a very useful technique to evaluate the mechanical properties of the actual irradiated fuel.

4. Conclusion

The simulated fuel with the burnup of 150 GWd/t was prepared and the nanoindentation tests were performed for the fuel. In the simulated fuel, the matrix phase and the oxide precipitates have the fluorite and perovskite-type structure. The nanoscale mechanical properties of the matrix phase and oxide precipitates existed in the simulated fuel

surface can be measured by the nanoindentation. The values of the mechanical properties of the matrix phase are higher than those of the oxide precipitates. The mean values of the reduced modulus and nanohardness of the matrix phase are 217 ± 20 GPa and 10.9 ± 1.5 GPa, respectively. The mean values of the reduced modulus and nanohardness of the oxide precipitates are 197 ± 17 GPa and 8.2 ± 0.5 GPa, respectively.

References

[1] T. Muromura, T. Adachi, H. Takeishi, Z. Yoshida, T. Yamamoto, K. Ueno, J. Nucl. Mater. 151 (1988) 318.
[2] T. Adachi, T. Muromura, H. Takeishi, T. Yamamoto, J. Nucl. Mater. 160 (1988) 81.
[3] P.G. Lucuta, R.A. Verral, Hj. Matzke, B.J. Palmer, J. Nucl. Mater. 178 (1991) 48.
[4] K. Une, M. Oguma, J. Nucl. Sci. Technol. 20 (1983) 844.
[5] P.G. Lucuta, Hj. Matzke, R.A. Verral, J. Nucl. Mater. 223 (1995) 51.
[6] Hj. Matzke, P.G. Lucuta, R.A. Verrall, J. Henderson, J. Nucl. Mater. 247 (1997) 121.
[7] W.C. Oliver, G.M. Pharr, J. Mater. Res. 7 (1992) 1564.
[8] M. Nishibori, K. Kinoshita, Thin Solid Films 48 (1978) 325.
[9] D. Newey, M.A. Wilkins, H.M. Pollock, J. Phys. E: Sci. Instrum. 15 (1982) 119.
[10] J.B. Pethica, in: V. Ashworth, W. Grant, R. Procter (Eds.), Ion Implantation into Metals, Pergamon Press, Oxford, 1982, p. 147.
[11] J.B. Pethica, R. Hutchings, W.C. Oliver, Philos. Mag. A 48 (1983) 593.
[12] K. Kurosaki, Y. Saito, H. Muta, M. Uno, S. Yamanaka, J. Alloys Compd. 381 (2004) 240.
[13] K. Kurosaki, D. Setoyama, J. Matsunaga, S. Yamanaka, J. Alloys Compd. 386 (2004) 261.
[14] M.J. Bell, ORIGEN-2 Code, Oak Ridge National Laboratories, Report ORNL-TM4397, 1973.
[15] F.K. Mante, G.R. Baran, B. Lucas, Biomaterials 20 (1999) 1051.
[16] T.F. Page, W.C. Oliver, C.J. McHargue, J. Mater. Res. 8 (1993) 1028.
[17] W.D. Nix, H. Gao, J. Mech. Phys. Solids 46 (1998) 411.
[18] M. Hirai, in: Proceedings of Fall Meeting of Atomic Energy Society of Japan, October 2-5, Sendai, Japan, F58, 1985.
[19] K. Yamada, S. Yamanaka, T. Nakagawa, M. Uno, M. Katsura, J. Nucl. Mater. 247 (1997) 289.